





## Article

# Biosynthesized ZnO-NPs Using Sea Cucumber (*Holothuria impatiens*): Antimicrobial Potential, Insecticidal Activity and *In Vivo* Toxicity in Nile Tilapia Fish, *Oreochromis niloticus*

Mostafa A. Elbahnasawy<sup>1</sup>, Hussein A. El-Naggar<sup>2</sup>, Ibrahim E. Abd-El Rahman<sup>3</sup>, Mohamed H. Kalaba<sup>1</sup> , Saad A. Moghannem<sup>1</sup> , Fatimah Al-Otibi<sup>4</sup>, Reham M. Alahmadi<sup>4</sup>, Othman F. Abdelzاهر<sup>2</sup>, Mohamed M. Mabrouk<sup>5</sup>, Ahmed G. A. Gewida<sup>5</sup> , Marwa F. AbdEl-Kader<sup>6</sup> and Ahmed I. Hasaballah<sup>2,\*</sup> 

<sup>1</sup> Botany and Microbiology Department, Faculty of Science, Al-Azhar University, Nasr City 11884, Egypt

<sup>2</sup> Zoology and Entomology Department, Faculty of Science, Al-Azhar University, Nasr City 11884, Egypt

<sup>3</sup> Department of Plant Protection, Faculty of Agriculture, Al-Azhar University, Cairo 32897, Egypt

<sup>4</sup> Department of Botany and Microbiology, College of Science, King Saud University, Riyadh 11451, Saudi Arabia

<sup>5</sup> Fish Production Department, Faculty of Agriculture, Al-Azhar University, Cairo 32897, Egypt

<sup>6</sup> Department of Fish Diseases and Management, Sakha Aquaculture Research Unit, Central Laboratory for Aquaculture Research, A.R.C., Kafrelsheikh 33516, Egypt

\* Correspondence: ahsience09@azhar.edu.eg



**Citation:** Elbahnasawy, M.A.; El-Naggar, H.A.; Abd-El Rahman, I.E.; Kalaba, M.H.; Moghannem, S.A.; Al-Otibi, F.; Alahmadi, R.M.; Abdelzاهر, O.F.; Mabrouk, M.M.; Gewida, A.G.A.; et al. Biosynthesized ZnO-NPs Using Sea Cucumber (*Holothuria impatiens*): Antimicrobial Potential, Insecticidal Activity and *In Vivo* Toxicity in Nile Tilapia Fish, *Oreochromis niloticus*. *Separations* **2023**, *10*, 173. <https://doi.org/10.3390/separations10030173>

Academic Editor: Stefania Garzoli

Received: 18 January 2023

Revised: 21 February 2023

Accepted: 22 February 2023

Published: 3 March 2023



**Copyright:** © 2023 by the authors. Licensee MDPI, Basel, Switzerland. This article is an open access article distributed under the terms and conditions of the Creative Commons Attribution (CC BY) license (<https://creativecommons.org/licenses/by/4.0/>).

**Abstract:** In this study, a sustainable and eco-friendly method was used to prepare zinc oxide nanoparticles (ZnO-NPs) using a sea cucumber aqueous extract. Then, ZnO-NPs were characterized by instrumental analysis (UV-vis, HR-TEM, XRD, FT-IR, and DLS) and evaluated for their possible antibacterial, antifungal, and insecticidal activities. Additionally, the toxicity of ZnO-NPs was evaluated *in vivo* against Nile Tilapia (*Oreochromis niloticus*). The sea cucumber was collected from the Gulf of Suez (Red Sea) at Al-Ain Al-Sokhna coast in Egypt and identified as *Holothuria impatiens*. The prepared *Hi*-ZnO-NPs peaked at 350 nm in UV-Vis spectral analysis. They showed quasi-spherical shaped particles with sizes ranging from 13 nm to 47 nm and a predominate size of 26 nm as indicated by HR-TEM. The XRD pattern of *Hi*-ZnO-NPs revealed a crystalline phase with an average size of 17.2 nm as calculated by Debye-Scherrer equation. FTIR analysis revealed the possible role of *H. impatiens* biological molecules in the biosynthesis process of ZnO-NPs. *Hi*-ZnO-NPs showed a negative zeta potential of  $-19.6$  mV, demonstrating moderate stability. Biosynthesized *Hi*-ZnO-NPs revealed broad antimicrobial activity against Gram-positive bacteria (*S. aureus* ATCC 25923 and *E. faecalis*), Gram-negative bacteria (*S. typhi*, *K. pneumonia* and *E. coli*), and filamentous fungi (*Aspergillus niger*). *Hi*-ZnO-NPs demonstrated larvicidal activity against the mosquito, *Culex pipiens* ( $LC_{50} = 2.756$  ppm and  $LC_{90} = 9.294$  ppm), and adulticidal action against the housefly, *Musca domestica* ( $LD_{50} = 4.285$  ppm and  $LD_{90} = 22.847$  ppm). Interestingly, *Hi*-ZnO-NPs did not show mortality effects against Nile tilapia fish (*Oreochromis niloticus*), highlighting the potential safety of *Hi*-ZnO-NPs to highly exposed, non-target organisms. However, histopathological and hematological investigations provided dose-dependent impacts of *Hi*-ZnO-NPs to Nile tilapia. Overall, data provide an eco-friendly approach for synthesizing novel *Hi*-ZnO-NPs with multiple biomedical properties and potentially low toxicity to Nile tilapia fish.

**Keywords:** biosynthesis; nanoparticles; zinc oxide; sea cucumber; *Holothuria impatiens*; antimicrobial activity; larvicidal; adulticidal; toxicity; Nile tilapia; *Oreochromis niloticus*

## 1. Introduction

Nanotechnology is a branch of science that deals with synthesis, characterization, modification, and application of nanosized materials in diverse fields. It has shown a very

rapid growth in fabrication of novel nanostructured materials with promising therapeutic uses in various medical applications. Due to the unique physicochemical properties and enhanced performance offered by nanosized materials, nanotechnology has reached almost all fields with outstanding applications [1]. Metal oxide nanoparticles particularly zinc-oxide nanoparticles (ZnO-NPs) have trended the field due to their properties and extensive interest and usage.

Marine environments are among the richest and most complex ecosystems in terms of biological and chemical diversity [2,3]. There is no doubt that the marine environment is a very rich source of bioactive molecules [4,5]. All of the progressive improvements in the past five decades of marine environment exploration have resulted in isolation of approximately 24,662 structurally unique new bioactive compounds from marine organisms [6]. Recently, most scientists focused on investigating invertebrates and their purified compounds against human pathogens. Among marine invertebrates, the sea cucumber (Class Holothuroidea) has shown economic importance as a tonic food and its involvement in folk medicine in Asia. Out of 1400 species of sea cucumbers all over the world, at least 60 species were harvested by artisanal and trawl fishing due to their commercial interests. *Holothuria impatiens* (Family: Holothuriidae) is a cryptic species and possesses a wide range of bioactive ingredients. Due to their importance, their abundance is a vital issue and attempts to culture them is highly recommended [7,8]. Tropical sea cucumber mariculture has the potential to become a commercial industry and contribute towards natural population restocking [8]. Nutritionally, sea cucumbers have an impressive profile of valuable nutrients such as vitamins, minerals and amino acids. They have many unique biological activities including antimicrobial, antioxidant, anticancer, anti-inflammatory, antihyperglycemic, anticoagulant, antihyperlipidemic, antihypertensive, and radioprotective [9,10].

Antimicrobial resistance is an urgent threat to global public health and development. The spreading of multi-drug resistance among community (outside hospitals)-associated bacteria is an additional threat and critical challenge to the global health [11,12]. However, increasing antimicrobial-resistant infections indicate that novel products are urgently needed to control antimicrobial-resistant microbes and reduce the emergence and spread of new forms of resistance outside hospitals [13]. Metal nanoparticles have been introduced as effective treatment platforms to fight life-threatening infections as they have shown activity against multidrug resistant bacteria *in vitro* [14–17]. Mosquitoes are the most important group of insects to public health as they transmit various diseases, such as malaria, filariasis, and dengue causing millions of deaths every year [18,19]. Among mosquitoes, *Culex pipiens* is the most common mosquito vector through urban and suburban areas of Africa. *C. pipiens* is the main vector of lymphatic filariasis. The house fly, *Musca domestica* (Diptera: Muscidae) is a well-known livestock pest of public health importance. It constitutes a worldwide problem wherever poor sanitation and bad hygienic conditions exist [20,21]. Moreover, the biology and ecology of dipterous flies make them ideal organisms to carry and disseminate human and animal pathogens such as helminth parasites, protozoan cysts, viruses, and bacteria [22]. Due to the developed resistance to chemical insecticides and their harmful side effects on non-target populations, investigating an alternative source with common insecticidal properties is needed. So, a marine environment may consider a rich source of novel compounds and derivatives with potential insecticidal properties that could alternate chemical insecticides.

In the present study, we synthesized ZnO-NPs using the aqueous extract of *Holothuria impatiens* (sea cucumber) as an ecofriendly, novel, and cost-effective approach. Biosynthesized *Hi*-ZnO-NPs were fully characterized, and evaluated for their antimicrobial, larvicidal, and adulticidal activities and potential toxicity toward Nile Tilapia fish (*Oreochromis niloticus* as a non-target model).

## 2. Materials and Methods

### 2.1. Sampling, Preservation and Identification of Sea Cucumber

Sea cucumber was collected during the spring season of 2021 by snorkeling at a one-meter depth in the Gulf of Suez (Red Sea) at Al-Ain Al-Sokhna coast in Egypt. Gulf of Suez is the northwestern arm of the Red Sea to the west of the Sinai Peninsula and it extends south-north from its mouth at the Strait of Jubal to its head at the city of Suez (314 km) and linked to the Mediterranean Sea by the vital shipping route, Suez Canal. After collection, specimens were washed with seawater and preserved in ice box containing ice cubes and a few pinches of table salt at  $-20\text{ }^{\circ}\text{C}$  until processing. Sea cucumber was identified as *Holothuria impatiens* on the basis of morphological characters [23–26].

### 2.2. *Holothuria Impatiens* Aqueous Extract Preparation

To prepare the aqueous extract, sea cucumber was extensively washed with tap water, chopped into small pits, homogenized (300 gm) with distilled water (250 mL) and methanol (250 mL) in a tightly closed jar, and stored in dark at  $-20\text{ }^{\circ}\text{C}$ . After one week, the mixture was filtered through a Whatman 542 filter paper [27].

### 2.3. Biosynthesis of ZnO-NPs Using *Holothuria Impatiens* Extract

To obtain cell debris-free extract, the aqueous extract of *H. impatiens* was filtered through a cotton filter, then centrifuged at 10,000 rpm for 15 min and the supernatant was collected. The collected extract was added at a ratio of 1:1 (*v/v*) to 1.5% (*w/v*) zinc acetate solution ( $\text{Zn}(\text{CH}_3\text{CO}_2)_2 \cdot 2\text{H}_2\text{O}$ , HiMedia, Mumbai, India), as a zinc precursor. The reaction mixture was adjusted to pH 7.0 and incubated for 72 h ( $37\text{ }^{\circ}\text{C}$ , 120 rpm, in dark) [28]. Biosynthesized *Hi-ZnO*-NPs were detected by the formation of cloudy color. *Hi-ZnO*-NPs were harvested by centrifugation (10,000 rpm for 15 min) and extensively washed with sterile deionized water to remove any leftover biological molecules. The purified *Hi-ZnO*-NPs were resuspended with sterile deionized water and dried at  $90\text{ }^{\circ}\text{C}$ . Before characterization, *Hi-ZnO*-NPs powder was resuspended in 10 mL deionized water [29].

### 2.4. Characterization of *Hi-ZnO*-NPs

*Hi-ZnO*-NPs were characterized according to Barzinjy and Azeez [30]. The UV-visible absorption spectra of *Hi-ZnO*-NPs were measured using a Hitachi U-2800 (290–710 nm). Fourier transform infrared spectroscopy (FTIR) spectra were taken in the  $400\text{--}4000\text{ cm}^{-1}$  range using an Agilent system Cary 630 FTIR model. The collected spectral data were compared to the reference chart to determine the functional groups present in the sample. High-resolution transmission electron microscopy (HR-TEM) (JEOL 2100, Tokyo, Japan) was used to examine the morphology of *Hi-ZnO*-NPs. X-ray diffraction (XRD) was used to study the crystalline structure of *Hi-ZnO*-NPs using the Shimadzu apparatus with nickel-filter and Cu-K $\alpha$  target (Shimadzu Scientific Instruments, Kyoto, Japan). Zeta potential of the nanoparticles in the solution was determined by Litesizer 500 (Anton Paar, Graz, Austria) using electrophoretic light scattering.

### 2.5. Antimicrobial Activities of *Hi-ZnO*-NPs

Microbial cultures of *Salmonella typhi*, *Klebsiella pneumonia*, *Escherichia coli*, *Staphylococcus aureus* ATCC 25923, *Enterococcus faecalis*, and *Aspergillus niger* were kindly provided by the Bacteriology Laboratory, Botany and Microbiology Department, Faculty of Science, Al-Azhar University. The antimicrobial activity was determined against bacteria and fungus (*A. niger*) on Muller Hinton agar (MHA) and potato dextrose agar (PDA), respectively. On the surface of prepared MHA and PDA, a 24-h-old culture of bacteria and a 7-day-old culture of fungus were cultured. A sterile cork borer was used to cut 8 mm wells; 100  $\mu\text{L}$  of *Hi-ZnO*-NPs suspension (5 mg/mL), aqueous extract of *H. impatiens*, and 1.5% (*w/v*) zinc acetate solution were applied to each well separately. Standard paper discs (6 mm) containing chloramphenicol 30  $\mu\text{g}$ /disc and fluconazole 25  $\mu\text{g}$ /disc were employed as controls for bacteria and fungi, respectively. The plates were left for 2 h at

4 °C followed by incubation for either 24 h at 37 °C (for bacteria) or 96 h at 28 °C (for fungi). The experiment was repeated three times, and the inhibition zones were measured and documented after incubation [31].

### 2.6. Insecticidal Bioassays of Hi-ZnO-NPs

Egg rafts of laboratory reared *Culex pipiens* mosquitoes were obtained from the colony established at Faculty of Science, Al-Azhar University, Cairo, Egypt. The hatched larvae were provided ad libitum with fish food as a diet. The house fly, *Musca domestica* (L.) adults used in the study were fed on sugar solution and water dissolved milk powder (10% w/v). Both tested insects were maintained at laboratory conditions of  $27 \pm 2$  °C,  $70 \pm 5\%$  relative humidity (RH), with 14–10 h photoperiod in the insectary of Medical Entomology, Faculty of Science, Al-Azhar University, Egypt [32,33]. For toxicity bioassays, preliminary experiments were conducted to estimate the appropriate range of concentrations for further application on both tested insects.

The larvicidal activity of biosynthesized Hi-ZnO-NPs against *Culex pipiens* was evaluated according to the World Health Organization protocol [34], with minor modifications. Briefly, twenty-five 3rd larval instar were subjected to serial concentrations of Hi-ZnO-NPs (0.5, 1, 2, 4, and 8 ppm), in five replicates with including a negative control (distilled water) and a positive control (1 ppm temephos). Larval mortality was recorded 24 h post-treatment to calculate lethal concentrations. Later, lethal concentrations (LC<sub>50</sub> and LC<sub>90</sub>) were determined and used for further non-target experiments. The adulticidal activity of the adult house fly (*Musca domestica*) was evaluated using the topical application method described by Wright [35]. Briefly, ten adults from both sexes (3-days old) were anesthetized with diethyl ether for 3 min then 1 µL of Hi-ZnO-NPs (doses: 0.5, 1, 2, 4, and 8 µg/adult) was applied by Hamilton microliter syringe 701-N (Sigma-Aldrich) on the dorsal thorax alongside with a negative control (distilled water) and Cypermethrin (Dethriod 10<sup>®</sup>, 10% w/v cypermethrin, Pentacheme Co. Ltd., Thailand) as a positive control at a concentration of 1 µL/adult. Each concentration was replicated five times. Adulticidal activity was recorded 24 h post-treatment.

### 2.7. Toxicity of Hi-ZnO-NPs

This experiment aimed to determine the potential hazards of biosynthesized Hi-ZnO-NPs to the non-target Nile Tilapia fish (*Oreochromis niloticus*). Apparently healthy sex-reversed (all male) fingerlings were purchased from a commercial hatchery in Sharkia Governorate, Egypt. The fingerlings were transported using a fish transport vehicle supplied with aeration tools. Fingerlings were adapted to the experimental condition for 15 days before starting the experiment. Four concentrations 10 times higher than the obtained LC<sub>50</sub> concentration for larval treatment (10, 20, 40, and 80 ppm) were applied against *O. niloticus* (average initial weight  $30.21 \pm 0.47$  g) in glass aquaria (40 × 25 × 30 cm) alongside with the controls in 3 replicates per each treatment according to Mount [36]. Each aquarium (5 fishes/aquarium) was filled with 20 Liter water and this level was maintained throughout the experimental period. All experimental aquaria were supplied with dechlorinated tap water through a water pipeline system supplied with an air pipeline using an air blower 2 HP.

#### 2.7.1. Water Quality Parameters

Several water parameters such as temperature, dissolved oxygen, pH and total ammonia concentration were recorded throughout the experiment period.

#### 2.7.2. Experimental Diet

All fish groups were fed on commercial diet contains ingredients with chemical composition as shown in Table 1. Fish were fed at the rate of 3% of body weight per day and food was daily provided at three time points (8, 12 and 15 h).

**Table 1.** Diet formulation and proximate analysis (g/kg).

Diet Ingredients (%)	
Fish meal	18.0
Soybean meal	29.0
Yellow corn	20.0
Wheat bran	15.0
Alfalfa hay	12.0
Sunflower oil	3.0
Minerals mixture	1.0
Vitamin mixture	1.0
Carboxymethyl cellulose	1.0
Total	100
Chemical Composition (g/kg)	
Crude protein	30.11
Ether extract	12.35
Ash	14.34
NFE <sup>1</sup>	43.20
GE <sup>2</sup>	4600 Kcal/kg

<sup>1</sup> NFE, nitrogen free extract = 100 – (CP + CF + EE + Ash%). <sup>2</sup> GE, gross energy calculated using the 5.65, 9.45, and 4 for CP, EE and NFE, respectively.

### 2.7.3. Histological and Hematological Assays

Tissue samples from the gills and the liver from *Hi-ZnO-NPs*-treated and untreated fish were fixed by formaldehyde (10%) for 24 h. After fixation, the tissues were dehydrated (in a series of ethanol/water washes of increasing concentrations), diaphonized, and embedded in plastic paraffin. Subsequently, 5 mm thick cuts were precisely made in automatic microtome. The sections were stained with hematoxylin-eosin [37].

Blood samples were collected from the caudal vertebral vein of an anaesthetized fish at the end of the feeding experiment then divided into two groups, one containing EDTA (as anticoagulant) for hematological examination, and the other without EDTA for serum investigations. Red blood cells (RBCs) and white blood cells (WBCs) were counted using hemocytometer and Natt-Herrick solution. Hemoglobin (Hb) concentration was determined using the cyanomet hemoglobin method Drabkin's solution. The micro hematocrit method was used for estimation of the packed cell volume (PCV) % to measure RBCs mass. Mean corpuscular volume (MCV), mean corpuscular hemoglobin (MCH), and mean corpuscular hemoglobin concentration (MCHC) were assessed. Differential leukocytic count (DLC) was calculated according to the following formula: Absolute DLC = no. of white cells X no. of total leukocytic count/100. Serum total proteins, albumins, aspartate aminotransferase, alanine aminotransferase, triglycerides, creatinine, cholesterol, glucose, urea were determined colorimetrically at their corresponding wavelengths. Globulins content was calculated mathematically. Superoxide dismutase, catalase, lipid peroxide, lipase, and amylase, was determined colorimetrically their corresponding wavelengths. Serum lysozyme was assayed by ELISA based on the ability of lysozyme to lyses Gram positive lysozyme sensitive bacterium; *Micrococcus lysodeikticus* (Sigma, USA) at the wavelength 450 nm. Immunoglobulin M (IgM) was measured by ELISA using a commercial kit (Bioneovan.co., Beijing, China).

### 2.8. Statistical Analysis

Mean and standard error (SE) were calculated for each treatment. Larval and adult mortality data were subjected to probit analysis to calculate LC<sub>50</sub>, LC<sub>90</sub>, LD<sub>50</sub>, and LD<sub>90</sub> at

95% confidence limits. ANOVA and *Chi*-square values were evaluated using SPSS (ver. 25). For pairwise comparisons, Tukey HSD post hoc test was applied. *p* value was considered significant at <0.05.

### 3. Results

#### 3.1. Identification of Sea Cucumber

Based on morphological characteristics, as shown in Figure 1, the collected sea cucumber was identified as *Holothuria* (*Thymiosycia*) *impatiens* (Forsskål, 1775). *H. impatiens* has shown a tough, brown spotted, elongated cylindrical shape with a tough tegument, prominent papillae, and a firm but pliable body. Its skin color is variegated grey, brown, or purplish-brown, with alternating bands of pale and dark color. Its skin surface is covered with conical spiky bumps to distinguish it from other close strains such as *H. hilla*. *H. impatiens* can be found in shallow reefs, hidden below rocks, in seagrasses, and in silty environments up to 30 m in depth. It is characterized by its crown of about twenty feeding tentacles at the anterior end.



**Figure 1.** Sea cucumber; *Holothuria impatiens*. Kingdom: Animalia, Phylum: Echinodermata, Class: Holothuroidea, Order: Holothuriida, Family: Holothuriidae, *Holothuria* (*Thymiosycia*) *impatiens* (Forsskål, 1775).

#### 3.2. Characterization of Biosynthesized *Hi-ZnO-NPs*

Visual observation of the reaction mixture of *H. impatiens* extract and zinc acetate solution provided preliminary proof for the formation of *Hi-ZnO-NPs*. This was indicated by the appearance of a cloudy to milky-colored mixture, followed by the development of white to off-white precipitates at the bottom of the flasks. UV-Vis spectroscopy of a colloidal solution containing *Hi-ZnO-NPs* was screened in the range of 290–710 nm to confirm the reduction of  $Zn^{2+}$  to *Hi-ZnO-NPs*. The UV-Vis spectra of the *Hi-ZnO-NPs* sample revealed a prominent peak at 350 nm, which is a characteristic feature of zinc oxide nanoparticles (Figure 2A). The morphology of *Hi-ZnO-NPs* was examined by High-Resolution Transmission Electron Microscopy (HR-TEM) and showed quasi-spherical shaped particles with a broad size distribution (13–47 nm, the predominate size was 26 nm, and the average particle size was  $26.95 \pm 8.63$  nm). HR-TEM images revealed that the majority of the particles exist separately, however, certain HR-TEM images show few aggregated particles (Figure 2B,C).

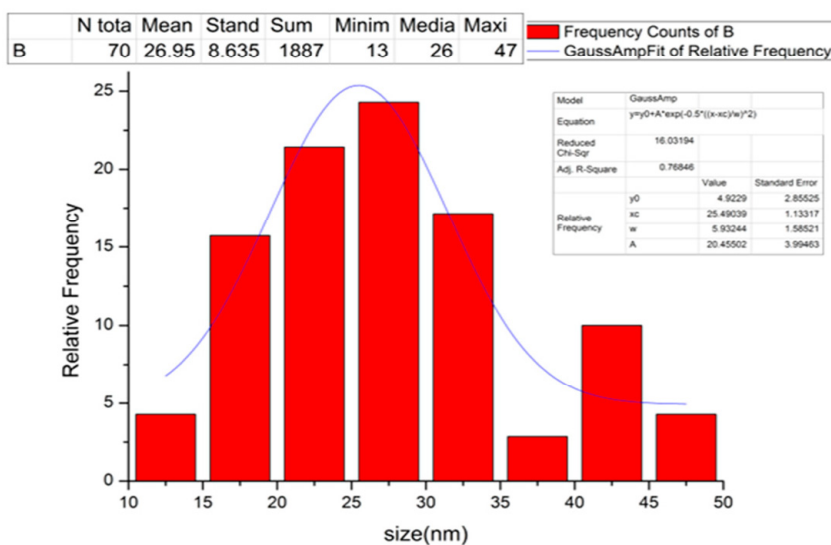
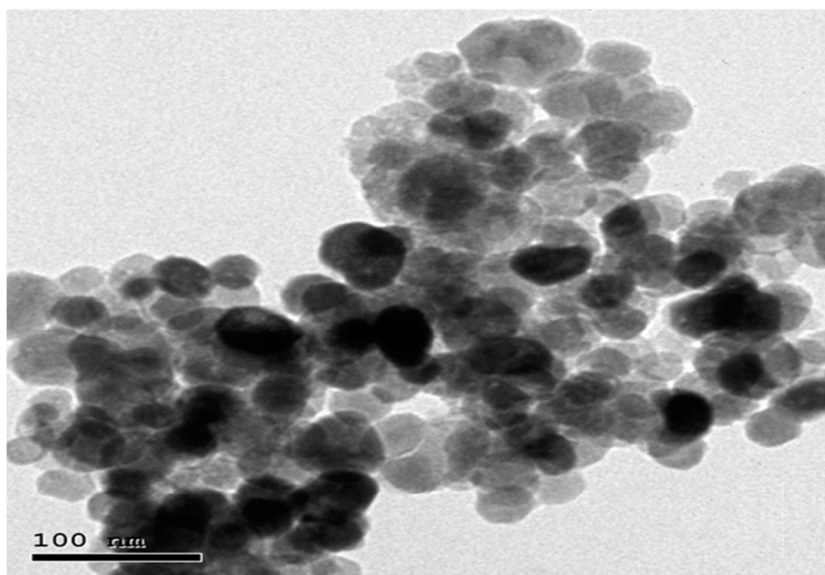
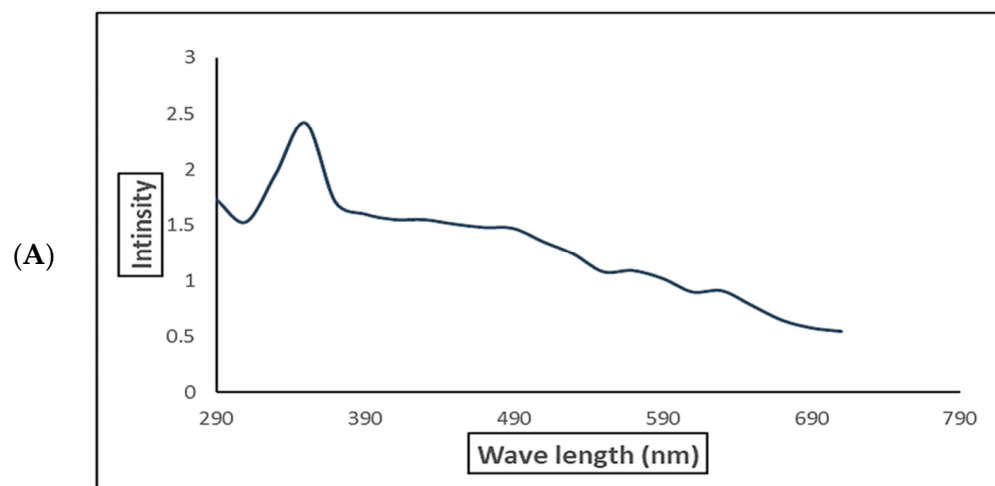
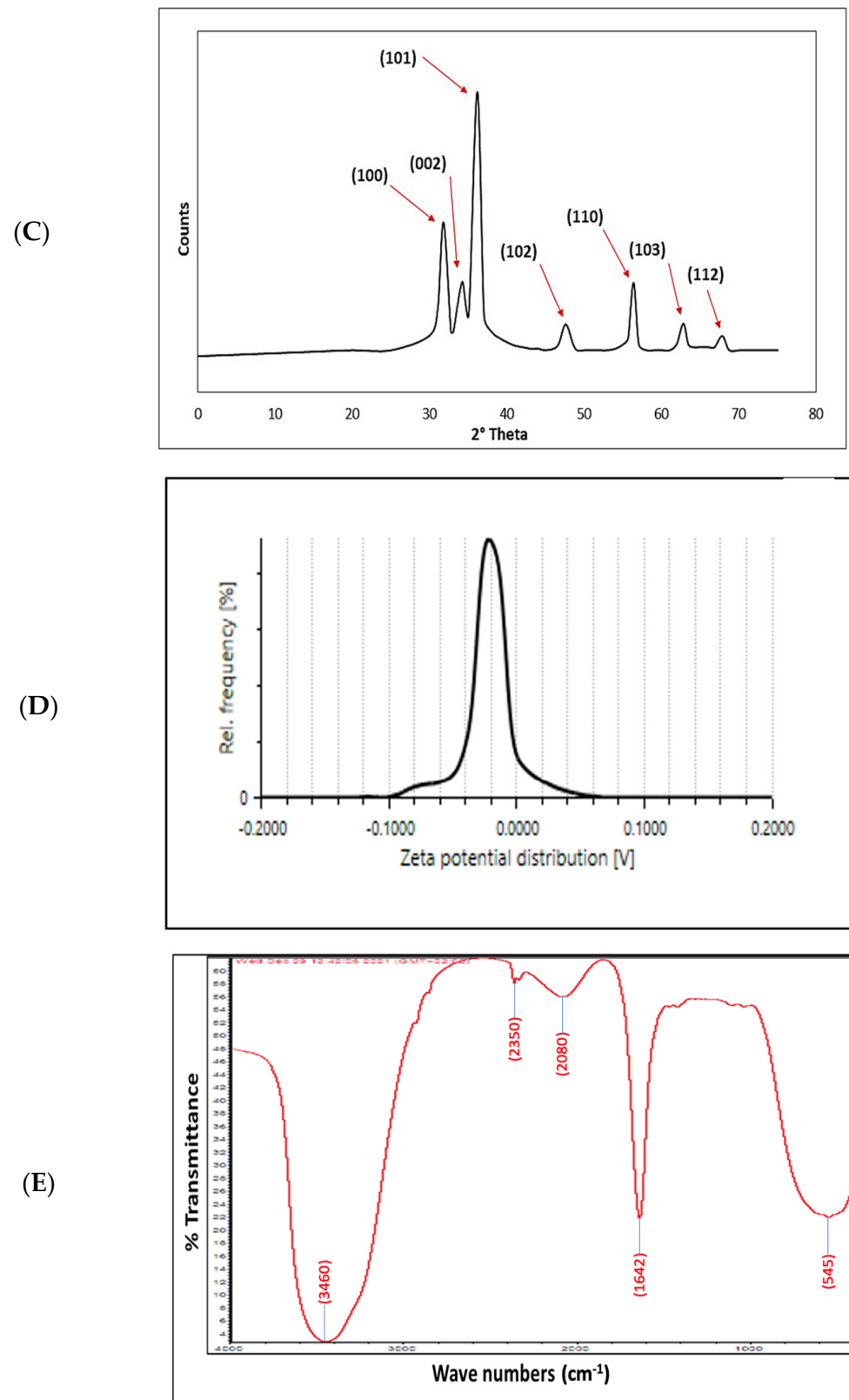


Figure 2. Cont.



**Figure 2.** Characterization of Hi-ZnO-NPs mediated by *Holothuria impatiens* aqueous extract. (A) UV-visible spectrum of Hi-ZnO-NPs. (B) HR-TEM image and size distribution chart of Hi-ZnO-NPs. (C) XRD pattern of Hi-ZnO-NPs. (D) Zeta potential of Hi-ZnO-NPs. (E) FTIR of Hi-ZnO-NPs.



X-ray diffraction (XRD) pattern indicated a crystallite phase of *Hi-ZnO-NPs* with an average size of 17.2 nm based on the Debye–Scherrer equation. The XRD profile also revealed strong and prominent peaks at 31.74, 34.17, 36.11, 47.52, 56.32, 62.76, and 67.79, which were categorized as planes (100), (002), (101), (102), (110) (103), and (112) (Figure 2D). These peaks corresponded well with wurtzite ZnO criteria from the Joint Committee on Power Diffraction (JCPD), file number (00-005-0664). Thus, the XRD pattern revealed that *Hi-ZnO-NPs* had a fine hexagonal crystalline structure which exhibited a good agreement with this reference model. Given the absence of any other distinct diffraction peaks, the formed *Hi-ZnO-NPs* were free of impurities and with a high phase purity. Zeta potential value of *Hi-ZnO-NPs* in colloidal solution has shown a negative zeta potential of −19.6 mV, indicating a moderate stability (Figure 2E). Fourier transform infrared spectroscopy (FTIR) was used to investigate the potential role of biological molecules from *H. impatiens* aqueous extract in the synthesis of *Hi-ZnO-NPs*. The findings showed substantial absorption spectra ranging from 400 to 4000 cm<sup>−1</sup> (Figure 2F) with existence of an absorption band at 545 cm<sup>−1</sup>, a sharp peak at 1642 cm<sup>−1</sup>, a weak absorption at 2080 cm<sup>−1</sup> and a peak at 3460 cm<sup>−1</sup>.

### 3.3. Antimicrobial Activities of Biosynthesized *Hi-ZnO-NPs*

The antimicrobial efficacy of *Hi-ZnO-NPs* was evaluated against Gram-positive bacteria (*S. aureus* ATCC 25923 and *E. faecalis*), Gram-negative bacteria (*S. typhi*, *K. pneumonia*, and *E. coli*), as well as filamentous fungi (*A. niger*). The data represented in (Table 2 and Figure 3) showed that *Hi-ZnO-NPs* have antimicrobial activities against all investigated microorganisms, with inhibition zones ranging from 22 nm to 30 mm.

**Table 2.** Antimicrobial potential of biosynthesized *Hi-ZnO-NPs*.

Microorganism	Mean ± SD of Inhibition Zone Diameter (mm) of the Tested Compounds			
	<i>Hi-ZnO-NPs</i> (NPs)	Aqueous Extract of Sea Cucumber (F)	Zinc Acetate Solution (S)	Antibiotic Control (C)
<i>S. typhi</i>	22.3 ± 0.88	0	0	23.3 ± 0.88
<i>K. pneumonia</i>	27.0 ± 1.15	0	0	14.3 ± 0.88
<i>E. coli</i>	29.0 ± 0.57	0	0	0
<i>S. aureus</i> ATCC 25923	30.3 ± 0.33	0	0	27.3 ± 0.33
<i>E. faecalis</i>	29.3 ± 0.88	0	0	21.6 ± 0.33
<i>A. niger</i>	23.6 ± 1.45	0	0	0

On one side, *H. impatiens* extract and precursor solution (zinc acetate) did not show any activity against the examined microorganisms. On the other side, Chloramphenicol, a standard antibiotic, had a considerable effect on both *S. typhi*, *S. aureus* ATCC 25923 and *E. faecalis*, with inhibition zones ranging from 21 nm to 27 mm. It also had an intermediate activity (inhibition zone = 14 mm) on *K. pneumonia*, but not on *E. coli*. Furthermore, there was no action seen by fluconazole, which was utilized as the standard antifungal in this study, against *A. niger*.

### 3.4. Insecticidal Assay of Biosynthesized *Hi-ZnO-NPs*

Data obtained in (Tables 3 and 4) exhibited a gradual increase in mortality of tested *Hi-ZnO-NPs* against both tested insects. For *C. pipiens* larvae, tested materials were extremely effective against the 3rd larval instar. The maximum toxicity level was reached when 8 ppm concentration of *Hi-ZnO-NPs* was applied, while the lowest toxicity was obtained when 0.5 ppm concentration was applied. The recorded LC<sub>50</sub> value (2.756 ppm) and the LC<sub>90</sub> value (9.294 ppm) was calculated 24 h post exposure. These results were significantly different among tested concentrations (*d. f.* = 4, *p* < 0.05 and  $\chi^2$  = 23.943) except those of 0.5 ppm. Zinc acetate solution did not exhibit any larval mortality.

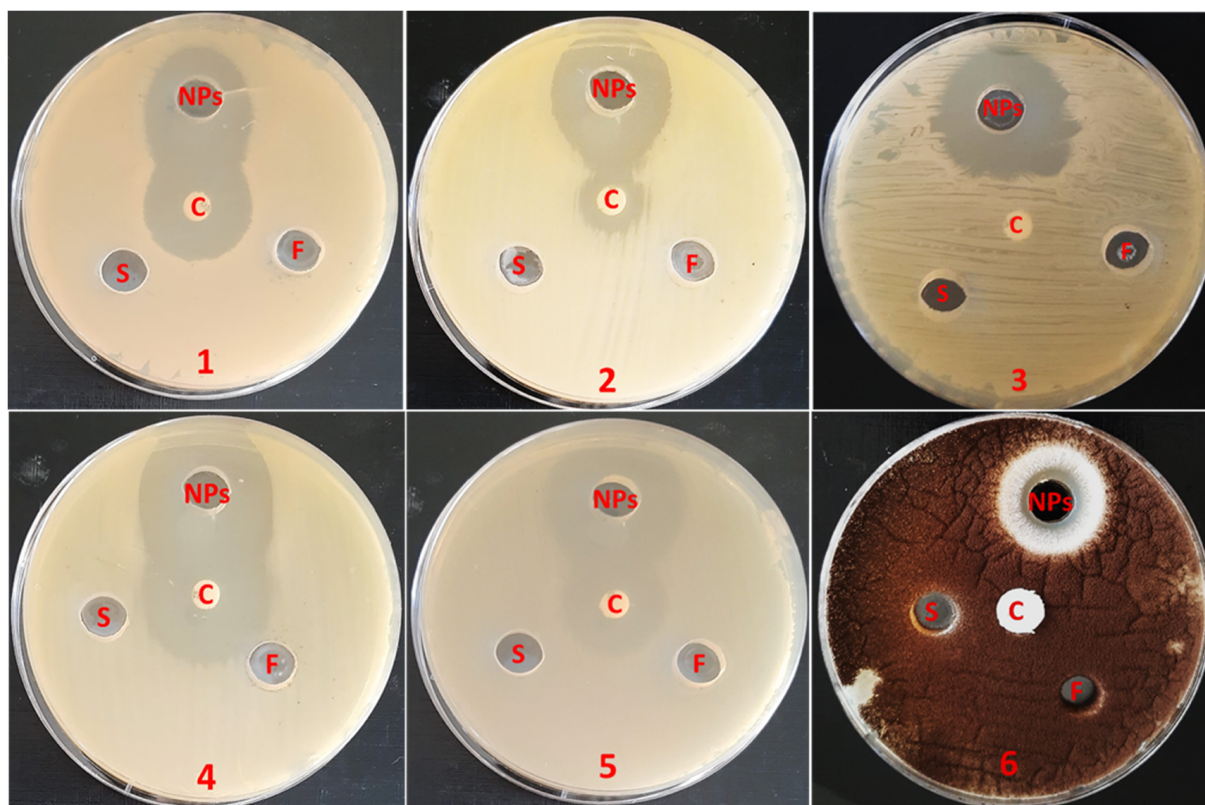


**Figure 3.** Antimicrobial activities of *Hi-ZnO-NPs* (NPs), *H. impatiens* aqueous extract (F), Zinc acetate solution (S), and standard antibiotics (C) against *S. typhi* (1); *K. pneumonia* (2); *E. coli* (3); *S. aureus* (4); *E. faecalis* (5), and *A. niger*, (6) using agar diffusion assay. Measurements were conducted in triplicates per each sample.

**Table 3.** Larvicidal activity of *Hi-ZnO-NPs* against the 3rd larval instar of the mosquito vector, *Culex pipiens*.

Concentrations (ppm)	<i>n</i>	Larval Mortality % ± (SE)	LC <sub>50</sub> (LCL–UCL) (ppm)	LC <sub>90</sub> (LCL–UCL) (ppm)	χ <sup>2</sup> ( <i>df</i> = 4)
Control	125	1.7 ± 0.97 a			
Temephos	125	100 ± 0.0 f			
0.5	125	6.3 ± 0.97 a	2.756 (2.463–3.103)	9.294 (7.644–11.897)	23.943 ns
1	125	16.8 ± 0.8 b			
2	125	29.6 ± 0.97 c			
4	125	55.2 ± 1.49 d			
8	125	96.0 ± 1.26 e			

Larval mortalities are presented as Mean ± SE of five replicates, *n* = sample size. Different letters are significantly different at (*p* < 0.05). (LC<sub>50</sub>) concentration that kills 50% of population, (LC<sub>90</sub>) concentration that kills 90% of population, (LCL) lower confidence limit, (UCL) upper confidence limit, (*df*) degree of freedom, (χ<sup>2</sup>) Chi-square, ns = not significant (*p* > 0.05). No mortalities were recorded in the group treated with ZnO-NPs (without *H. impatiens*).

**Table 4.** Adulticidal activity of *Hi-ZnO-NPs* against the housefly, *Musca domestica* adults.

Concentrations ( $\mu\text{g}/\text{Adult}$ )	<i>n</i>	Adult Mortality % $\pm$ (SE)	LD <sub>50</sub> (LCL–UCL) (ppm)	LD <sub>90</sub> (LCL–UCL) (ppm)	$\chi^2$ ( <i>df</i> = 4)
Control	50	2.0 $\pm$ 2.0 a			
Cypermethrin	50	100 $\pm$ 0.0 f			
0.5	50	6.0 $\pm$ 2.11 ab	4.285 (3.361–5.883)	22.847 (13.875–52.051)	5.852 ns
1	50	14.0 $\pm$ 2.45 b			
2	50	26.0 $\pm$ 1.58 c			
4	50	44.0 $\pm$ 2.45 d			
8	50	72.0 $\pm$ 2.0 e			

See footnote Table 3.

For *M. domestica*, topical assay revealed that tested materials greatly increased adult mortality with LD<sub>50</sub> value of (4.285  $\mu\text{g}/\text{adult}$ ) and LD<sub>90</sub> value of (22.847  $\mu\text{g}/\text{adult}$ ) calculated 24 h post exposure. These results were significantly different among tested concentrations (*d. f.* = 4, *p* < 0.05 and  $\chi^2$  = 5.852) except those of 0.5 ppm. The high chi-square values indicate the homogeneity of tested populations. Zinc acetate did not exhibit any adulticidal activity. In general, *C. pipiens* larvae were much more sensitive to our biosynthesized *Hi-ZnO-NPs* than the *M. domestica* adults.

### 3.5. Toxicity of Biosynthesized *Hi-ZnO-NPs*

A preliminary experiment was conducted to determine the potential hazards of biosynthesized *Hi-ZnO-NPs* against the non-target fish, *O. niloticus*, following chronic exposure. *Hi-ZnO-NPs* (10, 20, 40, and 80 ppm) did not show any mortality against the non-target model *O. niloticus*. Water parameters did not show any significant differences due to applied concentrations with average temperature of 22.61  $\pm$  1.04 °C, dissolved oxygen 5.64  $\pm$  0.46 mg/L, pH 7.10  $\pm$  0.23 and total ammonia concentration was 0.22  $\pm$  0.02 mg/L.

#### 3.5.1. Gill Histopathology

Histopathological study of the gills revealed ideal structural organization of the lamellae in the control group without pathological alterations. The alterations of gills of *Hi-ZnO-NPs*-treated *Nile tilapia*, *Oreochromis niloticus* were dose-dependent. Fish exposed to the lowest concentration of *Hi-ZnO-NPs* (10 ppm) showed several gill histopathological alterations, lamellar fusion, lamellar epithelium lifting, proliferation of filamentary epithelium. Hyperplasia of primary epithelial cells, necrosis, and strong lamellar epithelium lifting were observed in gills exposed to 20 ppm *Hi-ZnO-NPs*. Furthermore, 40 ppm *Hi-ZnO-NPs* resulted in some visible aberrations to the structure of the gill tissues manifested by filament epithelium proliferation, edema, aneurisms, and presence of some necrotic cells. Exposure of fish to high concentration of *Hi-ZnO-NPs* (80 ppm) revealed hyperplasia of primary epithelial cells, edema in the filamentary epithelium, necrotic cells, and wrinkles of primary lamellae (Table 5, Figure 4A–E).

#### 3.5.2. Liver Histopathology

In the control group, the liver displayed a normal architecture with no pathological abnormalities. Likewise to gills, the liver tissue changes of *Hi-ZnO-NPs*-treated fish were dose-dependent. The dose of 10 ppm *Hi-ZnO-NPs* revealed hepatopancreatic damage and cytoplasmic vacuolation, necrosis, and pyknotic nuclei. Fish exposed to 20 ppm showed hepatocellular necrosis and hepatic cord disarrangement, cytoplasmic vacuolation, and hemorrhage. The histological alterations in liver were more evident in fish group exposed to 40 ppm, where the nuclei were displaced to the cell periphery, stasis within the sinusoid’s capillaries were observed, and signs of extreme necrosis were evident.

Hepatocyte hypertrophy was detected in the fish group exposed to 80 ppm and stasis within the sinusoid's capillaries was infiltration by inflammatory cells and cytoplasmic vacuolation with extreme focal necrotic hepatocytes was observed (Table 6, Figure 5A–E).

**Table 5.** Histopathological lesions on gills of *Nile tilapia*, *O. niloticus* exposed to Hi-ZnO-NPs.

Type of Gill Change	Control	Treatments (ppm)			
		10	20	40	80
Lamellar fusion	-	++	+++	+	+
Epithelium lifting	-	+	++	+	+
Vasodilatation	-	-	+	-	++
Aneurisms	-	-	-	+	-
Edema	-	-	+	-	-
Necrosis	-	+	++	++	++
Hyperplasia	-	+	++	+	++

(-) not alterations found, (+) visible alterations, (++) medium alterations, and (+++) extreme alterations.

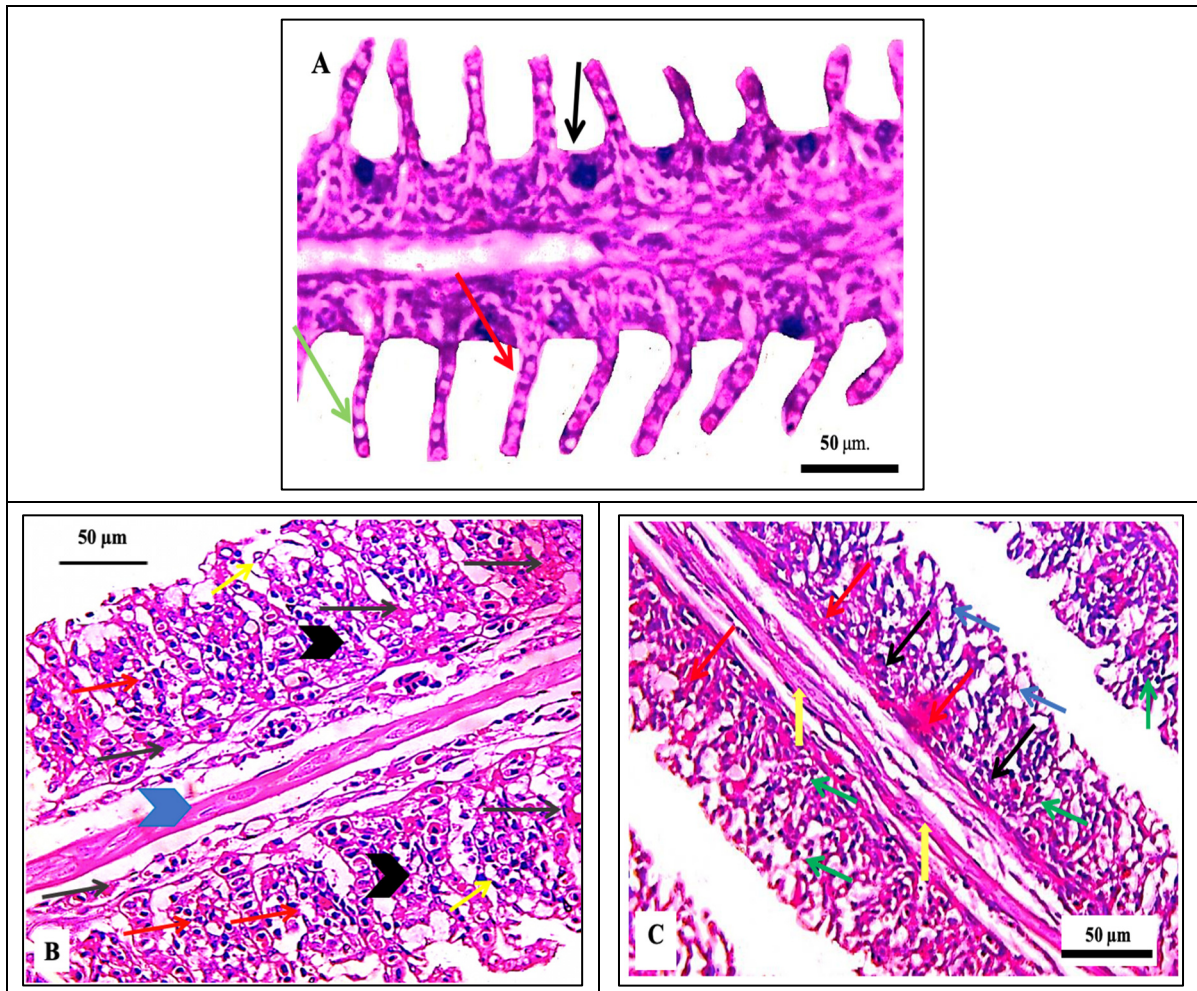


**Figure 4.** Cont.

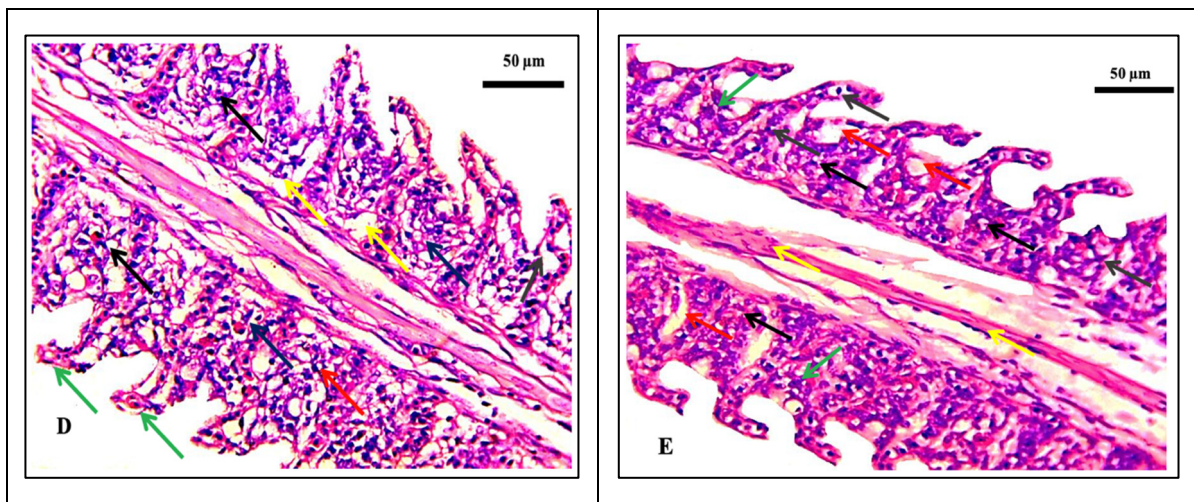


**Figure 4.** Photomicrographs of the gills of *Nile tilapia*, *O. niloticus* exposed to different concentrations of *Hi-ZnO-NPs*. (A) Gills of unexposed *Nile tilapia* (control) showing secondary lamellae (red arrow), primary lamellae (black arrow) and epithelial cells (green arrow) (B) Gills of *Hi-ZnO-NPs* (10 ppm)-treated *O. niloticus* showing induced Lamellar fusion (black arrow) lamellar lifting (yellow arrow), normal central venous sinus (blue arrow), congestion of blood vessels (brown arrow), proliferation of filamentar epithelium (red arrow). (C) Gills of *Hi-ZnO-NPs* (20 ppm)-treated *O. niloticus* demonstrating Hyperplasia (black arrow), necrosis (green arrow), lamellar epithelium lifting (blue arrow), vasodilatation (yellow arrow) and congestion of blood vessels (red arrow). (D) Gills of *Hi-ZnO-NPs* (40 ppm)-treated *O. niloticus* showing proliferation (black arrow), that in some instances conduced to lamellar fusion (purple arrow), edema (yellow arrow), Aneurisms in the apical region of the lamellar vascular axis (green arrow), epithelium lifting (brown arrow) and presence of some necrotic cells (red arrow). (E) 80 ppm *Hi-ZnO-NPs* treatment showing gills with hyperplasia (green arrow), edema (red arrow), extreme dilation of the central venous (yellow arrow), proliferation of filamentar epithelium (black arrow) and necrotic cells in the primary secondary lamella (brown arrow). Stain H&E. Bar = 50 µm.

**Table 6.** Histopathological lesions recorded on the liver *Nile tilapia*, *O. niloticus* exposed ZnO-NPs.

Type of Liver Change	Control	Treatments (ppm)			
		10	20	40	80
Cytoplasmic vacuolation	-	+	+++	+	++
Hemorrhage	-	+	++	+	+
Pyknotic nuclei	-	+	+	+	+
Necrosis	-	+	+	++	++

(-) not alterations found, (+) visible alterations, (++) medium alterations, and (+++) sever alterations.

### 3.5.3. Hematological Parameters

*Hi-ZnO-NPs*-treated fishes revealed decreased levels of RBCs, WBCs, Hb, PCV, lymphocytes, and monocytes in comparison to the control group, while heterophil counts were nearly similar in all groups (Tables 7–10). Also, *Hi-ZnO-NPs*-treated fishes showed decreased serum total protein, albumin, globulin, triglycerides, and digestive enzymes (amylase and lipase) levels and increased glucose, cholesterol levels, AST, ALT, Urea, and creatinine levels. SOD and CAT levels were also increased by exposure of fishes to *Hi-ZnO-NPs*.

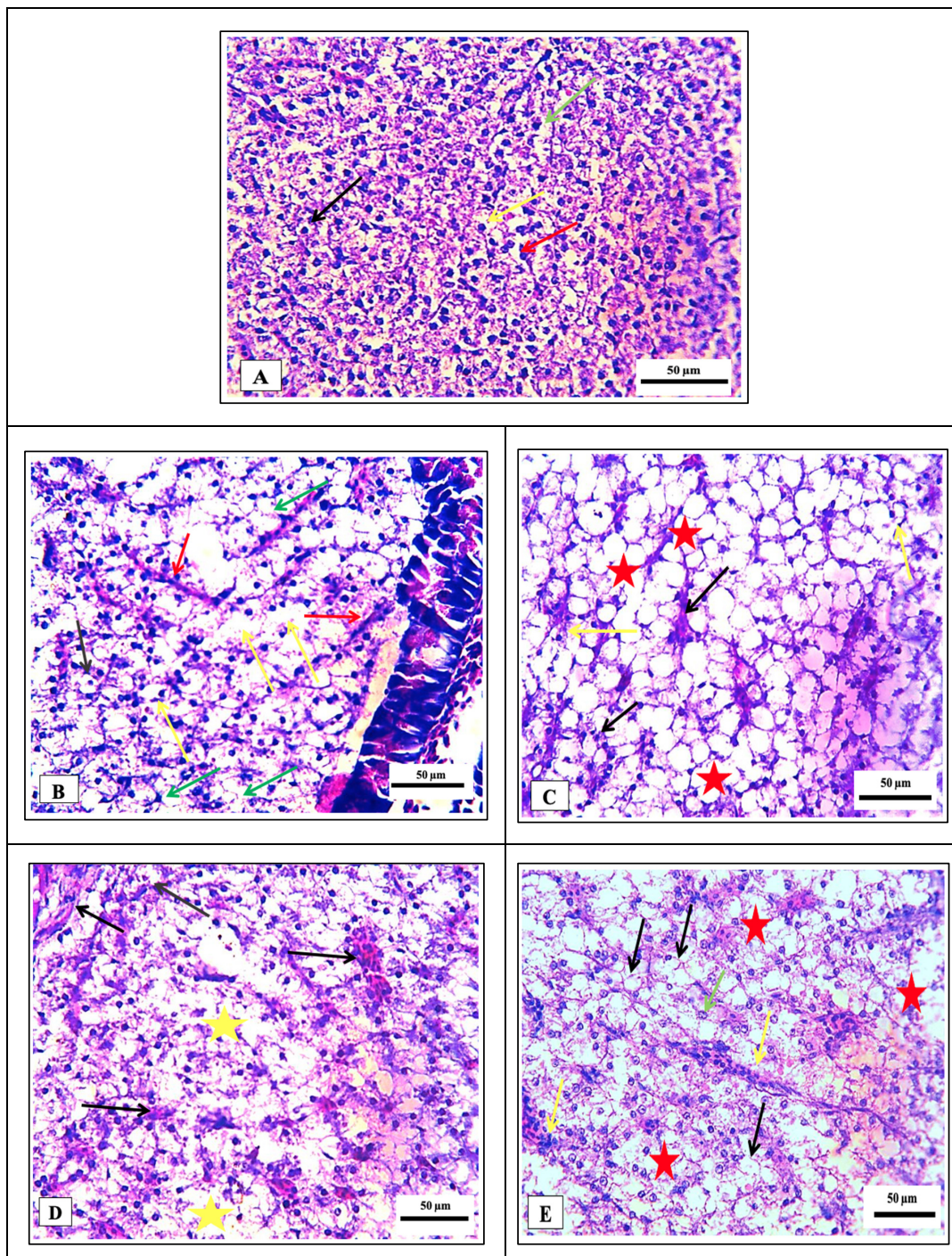


**Figure 5.** Photomicrographs of the liver of *Nile tilapia*, *O. niloticus* exposed to different concentrations of *Hi-ZnO-NPs*. (A) Unexposed (Control) liver showing hepatocyte (black arrow), spherical nucleus (yellow arrow), sinusoids (red arrow) and kupffer cells (green arrow). (B) Liver of *Hi-ZnO-NPs* (10 ppm)-treated *O. niloticus* showing cytoplasmic vacuolation (green arrow) necrosis (yellow arrow), pyknotic nuclei (brown arrow) and hemorrhage (red arrow). (C) 20 ppm treatment showing hepatocellular necrosis (yellow arrow), extreme cytoplasmic vacuolation (red star), and hemorrhage (black arrow). (D) 40 ppm treatment showing nuclei displaced to the cell periphery, stasis within the sinusoid's capillaries (black arrow) necrosis (yellow star). (E) 80 ppm treatment showing hepatocyte hypertrophy (green arrow) and stasis within the sinusoid's capillaries infiltrated by inflammatory cells (yellow arrow) and cytoplasmic vacuolation (black arrow) with sever focal necrotic hepatocytes (red star). Stain H&E. Bar = 50 µm.

**Table 7.** Hematological parameters of the *Nile tilapia*, *O. niloticus* exposed to different concentrations of biosynthesized *Hi-ZnO-NPs*.

Parameters	Treatments (ppm)				
	0	10	20	40	80
RBCs ( $\times 10^3/\text{mm}^3$ )	4.12	2.87	3.16	3.05	2.98
Hb (g/100 mL)	12.6	8.64	9.5	9.12	9.11
PCV (%)	40	28	31	30	29
MCV ( $\mu\text{m}^3/\text{cell}$ )	97.09	97.56	98.1	98.36	97.32
MCH (pg/cell)	30.58	30.1	30.06	29.9	30.57
MCHC (%)	31.5	30.86	30.65	30.4	31.41
WBCs ( $\times 10^3/\text{mm}^3$ )	10.76	9.33	8.68	9.15	10.25
Heterophil ( $\times 10^3/\text{mm}^3$ )	2.15	2.71	2.34	2.01	2.67
Lymphocyte ( $\times 10^3/\text{mm}^3$ )	7.53	5.6	5.38	6.22	6.56
Monocyte ( $\times 10^3/\text{mm}^3$ )	0.86	0.56	0.61	0.64	0.82
Basophil ( $\times 10^3/\text{mm}^3$ )	0.11	0.28	0.17	0.09	0.1
Esinophil ( $\times 10^3/\text{mm}^3$ )	0.11	0.19	0.17	0.18	0.1

**Table 8.** Immune responses of the *Nile tilapia*, *O. niloticus* exposed to different concentrations of biosynthesized *Hi-ZnO-NPs*.

Parameters	Treatments (ppm)				
	0	10	20	40	80
lysozyme ( $\mu\text{g}/\text{mL}$ )	6.29	3.98	4.29	4.19	4.25
phagocytic index (%)	1.3	1.02	1.01	1	1.05
phagocytic activity (%)	12.24	8.05	7.94	8.3	9.11
IgM ( $\mu\text{g}/\text{mL}$ )	5.26	1.35	2.58	3.01	4.15

**Table 9.** Serum biochemical measurements of the *Nile tilapia*, *O. niloticus* exposed to different concentrations of biosynthesized *Hi-ZnO-NPs*.

Parameters	Treatments (ppm)				
	0	10	20	40	80
Total protein (g/dL)	4.19	3.41	3.46	2.98	3.7
Albumin (g/dL)	1.66	1.39	1.33	1.21	1.41
Globulin (g/dL)	2.53	2.02	2.13	1.77	2.29
AST (U/L)	30.11	51.25	49.68	53.15	39.86
ALT (U/L)	30.16	41.03	38.46	50.14	37.98
Urea (mg/dL)	2.19	3.05	3.16	3.12	3.2
Creatinine (mg/dL)	0.4	0.61	0.59	0.59	0.58
Lipase (U/L)	29.86	20.19	26.87	29.78	29.65
Amylas (U/L)	61.01	40.16	42.85	51.39	46.82
Glucose (mg/dL)	10.25	11.35	15.99	12.34	10.98
Cholestrol (mg/dL)	69.86	74.34	91.34	81.64	80.15
Triglyceride (mg/dL)	103.15	81.34	85.99	90.14	88.69

**Table 10.** Serum antioxidant biomarkers of the *Nile tilapia*, *O. niloticus* exposed to different concentrations of biosynthesized *Hi-ZnO-NPs*.

Parameters	Treatments (ppm)				
	0	10	20	40	80
MDA nmol/g	16.54	25.64	29.86	19.86	20.01
CAT U/gm	18.17	13.56	14.25	14.29	12.99
SOD U/gm	23.58	14.85	15.98	18.64	17.06

Treatment of *Nile tilapia* with *Hi-ZnO-NPs* resulted in decreased lysozyme activity, phagocytic, phagocytic index and IgM levels. There was a decrease in the RBCs count, PCV and hemoglobin concentration, beside slight changes in MCV, MCH and MCHC in all treated groups. This normocytic normochromic anemia may be due to the decrease in the life span of RBCs.

#### 4. Discussion

Biological substances (extracellular or intracellular) from various organisms can be used for fabrication of ZnO-NPs. Herein, aqueous Zn<sup>2+</sup> (zinc acetate solution) was converted to zinc nanoparticles due to oxidation-reduction of Zn<sup>2+</sup> by the biological compounds and functional groups present in the aqueous extract of sea cucumber *H. impatiens*. Biosynthesized *Hi-ZnO-NPs* were initially observed as a white haziness and then they precipitated [28]. *Hi-ZnO-NPs* peaked in the region of 350–390 nm of UV–Vis absorption spectroscopy. This was supported by several studies that showed the formation of ZnO-NPs with characteristic peaks in this region. For example, Yusof et al. [38] synthesized ZnO-NPs from *Lactobacillus plantarum* TA4 cell-free filtrate and the UV-Vis absorption spectrum analysis revealed an absorption peak at 350 nm. Zinc sulfate, when used as a precursor for the biosynthesis of ZnO-NPs from *Ficus carica* leaf extract, revealed an absorption band of 360 nm [39]. Additionally, a strong peak of 370 nm in the UV–Vis spectra of green-produced ZnO-NPs mediated by the algal extract was recorded by El-Belely et al. [40].

Morphologically, HR-TEM images showed that *Hi-ZnO-NPs* were quasi-spherical shaped particles with sizes that ranged from 13 nm to 47 nm and the majority of particles were 26 nm. Furthermore, HR-TEM images revealed that the generated *Hi-ZnO-NPs* were dispersed. The XRD pattern revealed a fine hexagonal crystalline structure of *Hi-ZnO-NPs*. Because the nanomaterials tend to self-aggregate owing to their surface charge, stability is a crucial parameter to consider while investigating materials. The stability of nanostructures is directly related to the zeta potential (surface potential) [41]. Therefore, zeta potential analysis was used to determine the surface charge of *Hi-ZnO-NPs* and demonstrated a mean zeta potential of −19.6 mV, indicating their moderate stability. A similar value (−20.9 mV) of zeta potential is obtained for ZnO-NPs synthesized using the leaf extract of *Cinnamomum tamala* [42]. Due to electrostatic repulsions between the single-charged NPs during dispersion, a high positive or negative value of zeta potential indicates higher physical stability. On the other hand, because of the attractive Van der Waals forces acting on them, particles with low zeta potential tend to coagulate or flocculate, probably leading to poor physical stability. According to Nithya and Kalyanasundharam [43], ZnO-NPs with zeta potential falling between 32.06 and 17.89 mV have a moderate level of stability. FTIR analysis showed existence of an absorption band at 545 cm<sup>−1</sup>, which is the distinctive indication of ZnO bonding (fingerprint), confirming that the produced materials were truly ZnO nanoparticles. The sharp peak at 1642 cm<sup>−1</sup> is due to the carbonyl (C=O) stretching vibration of the amide I of proteins [15,44]. The weak absorption at 2080 cm<sup>−1</sup> is due to C≡C stretching vibration and the 2350 cm<sup>−1</sup> band is due to N–H stretching [45]. In addition, the peak at 3460 cm<sup>−1</sup> is due to vibration of stretch O–H in water, alcohol, and phenols [46].



In line with the observed antibacterial properties of *Hi-ZnO-NPs*, earlier investigations have demonstrated the antibacterial activity of ZnO-NPs against both Gram-positive and Gram-negative bacteria, as well as bacterial endospores [47,48]. The mechanism of antibacterial activity of ZnO nanoparticles could be through multiple ways, including the formation of reactive hydrogen species which have harmful effects against bacteria. Another mechanism includes that ZnO nanoparticles can bind to bacterial cell surfaces and subsequently enter inside to interact with cytoplasmic components [49,50]. In this study, *Hi-ZnO-NPs* exhibited antifungal activity against *A. niger*. According to He et al. [51], treatment of fungi with ZnO-NPs greatly decreased conidial production and distorted the conidiophores of *Penicillium expansum* and *Botrytis cinerea*, demonstrating antifungal capabilities. However, more studies are required to evaluate the activities of *Hi-ZnO-NPs* against more microorganisms, bacterial biofilms, and mammalian cell lines. Also, evaluating the minimum inhibitory concentration and minimum bactericidal concentration for *Hi-ZnO-NPs* are required. Based on the properties of *Hi-ZnO-NPs*, the shape and morphology of ZnO-NPs can affect their ability to penetrate microbial cells and cause damage to their membranes. Furthermore, the surface area of *Hi-ZnO-NPs* plays a crucial role in determining their antibacterial and antifungal activities, where ZnO-NPs with a large surface area are more effective for adsorbing on the microbial cell surface and disrupting cell membrane stability, leading to increased antimicrobial activity. It is important to note that the surface charge of ZnO-NPs can also affect their antimicrobial activities. ZnO-NPs with a positive surface charge exhibit stronger antimicrobial activities against Gram-negative bacteria than Gram-positive bacteria compared to particles with a negative surface charge and vice versa. The high negative charges on surfaces of Gram-negative bacteria enable them to bind strongly with the positively charged ZnO-NPs, while negatively charged ZnO-NPs tend to bond more to cell surfaces of Gram-positive bacteria [52,53].

A gradual increase in mortalities of *C. pipiens* larvae (*d. f.* = 4,  $p < 0.05$  and  $\chi^2 = 23.943$ ) and *M. domestica* adults (*d. f.* = 4,  $p < 0.05$  and  $\chi^2 = 5.852$ ) was observed after treatment with *Hi-ZnO-NPs* and the rate of mortalities was concentration/dose-dependent. The high chi-square values indicate the homogeneity of tested populations. Zinc acetate and ZnO-NPs (alone) revealed no mortality. In general, *C. pipiens* larvae were more sensitive to our biosynthesized *Hi-ZnO-NPs* over the *M. domestica* adults. Concentration-dependent mortality results obtained here were also reported in several previous studies. Hasaballah et al. [32] found highly toxic effects of synthesized *Spongia officinalis* ZnO-NPs with LC<sub>50</sub> of 31.82 ppm against *C. pipiens* larvae. Additionally, potent insecticidal activity of the soft coral, *Ovabunda macrospiculata* ZnO-NPs against *M. domestica* with LC<sub>50</sub> of 22.595 ppm was also reported [54]. Such results suggest that biosynthesized *Hi-ZnO-NPs* from natural origins such as marine organisms could exert larvicidal/adulticidal activities through the small size of NPs that makes it easily penetrate the insect cuticle.

The *in vivo* toxicity of biosynthesized *Hi-ZnO-NPs* were evaluated in the non-target model, *Nile tilapia* fish (*O. niloticus*) through histopathological investigations of gills and livers and hematological analyses. Concentrations of *Hi-ZnO-NPs* used in this experiment were 10 times higher than the obtained LC<sub>50</sub> concentration for larval treatment. Given their primary role in oxygen supply, any disturbance in gills would affect the fish's physiological and metabolic activities. Untreated fishes revealed ideal structural organizations of the lamellae without any pathological alterations, while *Hi-ZnO-NPs*-treated fishes showed dose-dependent histopathological alterations in their gills. Comparable findings in the gills of different fish species were also observed by Cengiz and Unlu [55]. They reported changes in structure of the gill and gut tissues of mosquitofish (*Gambusia affinis*) upon treatment with sublethal concentrations of commercial Deltamethrin (insecticide recommended by WHO). Additionally, Tilak et al. [56] reported bulging in the tips of primary gill lamellae, club shaped secondary gill lamellae, extreme necrotic changes in the epithelial cells, atrophy and fusion of gill lamellae in the fish exposed to Fenvalerate (a synthetic pyrethroid insecticide). Liver tissue investigation of fishes exposed to *Hi-ZnO-NPs* revealed dose-dependent hepatopancreatic damage, cytoplasmic vacuolation, necrosis and pyknotic

nuclei, and some other alterations compared to the control group. Similar results were obtained by Ikele et al. [57], they reported necrosis and pyknotic nuclei in the liver of fish exposed to Diethyl phthalate (DEP) (a synthetic phthalate ester with multiple applications, including as an insecticide). In another study, hyperplasia and focal necrosis were seen in the liver of Rohu fish (*Labeo rohita*) exposed to Carbofuran and Cypermethrin (both are synthetic insecticides widely used around the world) [58].

Some hematological parameters such as RBCs, Hb, PCV, WBCs, lymphocytes, monocytes, serum total protein, albumin, globulin, and triglycerides were decreased in *Nile tilapia* fish treated with *Hi-ZnO-NPs*. Digestive enzymes, ALT, AST, lysozyme activity, phagocytic, phagocytic index, and IgM levels were found to be affected by *Hi-ZnO-NPs* treatment in comparison to the control group. In harmony with these findings, Kaya et al. [59] found similar levels in the *Nile tilapia* during exposure to 1 mg/L of ZnO-NPs. Additionally, ZnO nanoparticles are reported to induce cytotoxic effects in zebrafish embryo and larval cell lines [60,61] which attributed to the increased production of reactive oxygen species (ROS) that overwhelms the intracellular stress and cell death. Overproduction of ROS exhausts the cellular antioxidants, and this effect may be implicated in ZnO-NPs poisoning in aquatic organisms including *Nile tilapia* fish [62]. ALT and AST are important parameters to identify the health status of fish as they play a major role in protein and amino acid metabolism, and changes of these two enzymes are indicators of cellular damage. Overall, although no mortality among the non-target model were recorded, the histopathological investigations and hematological parameters evaluation provided an in-depth analysis of the various side effects of our biosynthesized *Hi-ZnO-NPs*.

## 5. Conclusions

A sustainable and eco-friendly method was used to prepare zinc oxide nanoparticles (ZnO-NPs) using a sea cucumber (*Holothuria impatiens*) aqueous extract. *Hi-ZnO-NPs* were characterized by UV-Vis, HR-TEM, XRD, FT-IR, and DLS. Biosynthesized nanoparticles were stable, quasi-spherical, and with a predominant size at 17 nm. FTIR signature revealed the potential role of biological molecules from the *H. impatiens* aqueous extract in the synthesis of ZnO-NPs. *Hi-ZnO-NPs* showed wide antimicrobial activities against Gram-positive bacteria, Gram-negative bacteria, and filamentous fungi. They also induced potent larvicidal and adulticidal activities against *C. pipiens* and *M. domestica*, respectively. No mortality effects on the non-target model (*Nile tilapia* fish) after exposure to increasing doses of *Hi-ZnO-NPs*. Histopathological investigations and hematological parameters indicated dose-dependent impacts of *Hi-ZnO-NPs* to *Nile tilapia* fish. From a future perspective, using *Hi-ZnO-NPs* as a tool for controlling *C. pipiens* and *M. domestica* populations and combating microbial infections can be deeply studied for their action mechanisms and investigating the persistence and degradation of ZnO nanoparticles in the environment. Additionally, more *in vivo* toxicity studies of *Hi-ZnO-NPs* against multiple organisms are required. Furthermore, *Hi-ZnO-NPs* could be captured on other materials to avoid their release and spreading in the environment, thus decreasing any possible detrimental side effects on the environmental flora and organisms.

**Author Contributions:** Conceptualization, A.I.H. and M.A.E.; Formal analysis, A.I.H., M.A.E., F.A.-O., R.M.A. and I.E.A.-E.R.; Investigation, A.I.H., M.A.E., M.H.K., O.F.A., M.M.M., A.G.A.G., I.E.A.-E.R. and M.F.A.-K.; Methodology, A.I.H., M.A.E., H.A.E.-N., O.F.A., M.H.K., M.M.M., S.A.M., M.F.A.-K. and A.G.A.G.; Supervision, A.I.H. and M.A.E.; Visualization, O.F.A., S.A.M., I.E.A.-E.R., F.A.-O., R.M.A. and H.A.E.-N.; Writing—original draft preparation, A.I.H., M.A.E., M.H.K., H.A.E.-N., O.F.A., I.E.A.-E.R., F.A.-O., R.M.A., M.M.M., A.G.A.G. and M.F.A.-K.; Writing—review and editing, A.I.H., F.A.-O., R.M.A., M.H.K. and M.A.E. All authors have read and agreed to the published version of the manuscript.

**Funding:** The study was funded by the Researchers Supporting Project number (RSP2023R114), King Saud University, Riyadh, Saudi Arabia.

**Institutional Review Board Statement:** The animal study protocol was approved by the Institutional Aquatic Animal Care and Use Committee at Kafrelsheikh University (IAACUC-KSU-130-2022).

**Informed Consent Statement:** Not applicable.

**Data Availability Statement:** We will provide all data generated in this study upon request.

**Acknowledgments:** The authors extend their appreciation to the Researchers Supporting Project number (RSP2023R114), King Saud University, Riyadh, Saudi Arabia, and to the Faculty of Science, Al-Azhar University for supporting this work.

**Conflicts of Interest:** The authors declare no conflict of interest.

## References

1. Chausali, N.; Saxena, J.; Prasad, R. Recent trends in nanotechnology applications of bio-based packaging. *J. Agri. Food Res.* **2022**, *7*, 100257. [[CrossRef](#)]
2. Mona, M.H.; El-Naggar, H.A.; El-Gayar, E.E.; Masood, M.F.; Mohamed, E.N.E. Effect of human activities on biodiversity in Nabq Protected Area, South Sinai, Egypt. *Egypt. J. Aquat. Res.* **2019**, *45*, 33–43. [[CrossRef](#)]
3. Farrag, M.M.S.; El-Naggar, H.A.; Abou-Mahmoud, M.M.A.; Alabssawy, A.N.; Ahmed, H.O.; Abo-Taleb, H.A.; Kostas, K. Marine biodiversity patterns off Alexandria area, southeastern Mediterranean Sea, Egypt. *Environ. Monit. Assess.* **2019**, *191*, 367. [[CrossRef](#)] [[PubMed](#)]
4. El-Naggar, H.A.; Salem, E.-S.S.; El-Kafrawy, S.B.; Bashar, M.A.E.; Shaban, W.M.; El-Gayar, E.E.; Ahmed, H.O.; Ashour, M.; Abou-Mahmoud, M.E. An integrated field data and remote sensing approach for impact assessment of human activities on epifauna macrobenthos biodiversity along the western coast of Aqaba Gulf. *Ecohydrology* **2021**, *15*, e2400. [[CrossRef](#)]
5. EL-Naggar, H.A.; Bashar, M.A.E.; Rady, I.; El-Wetidy, M.S.; Suleiman, W.B.; Al-Otibi, F.O.; Al-Rashed, S.A.; Abd El-Maoula, L.M.; Salem, E.S.; Attia, E.M.H.; et al. Two Red Sea Sponge Extracts (*Negombata magnifica* and *Callyspongia siphonella*) Induced Anticancer and Antimicrobial Activity. *Appl. Sci.* **2022**, *12*, 1400. [[CrossRef](#)]
6. Metwally, A.S.; El-Naggar, H.A.; El-Damhougy, K.A.; Bashar, M.A.E.; Ashour, M.; Abo-Taleb, H.A.H. GC-MS analysis of bioactive components in six different crude extracts from the Soft Coral (*Simularia maxim*) collected from Ras Mohamed, Aqaba Gulf, Red Sea, Egypt. *Egypt. J. Aquat. Biol. Fish.* **2020**, *24*, 425–434. [[CrossRef](#)]
7. Sun, H.; Liang, M.; Yan, J.; Chen, B. Nutrient requirements and growth of the sea cucumber, *Apostichopus japonicus*. In *Advances in Sea Cucumber Aquaculture and Management*; Lovatelli, A., Conand, C., Purcell, S., Uthicke, S., Hamel, J.-R., Mercier, A., Eds.; FAO: Rome, Italy, 2004; pp. 327–331.
8. Purcell, S.W.; Conand, C.; Samyn, Y. *Commercially Important Sea Cucumber of the World*; FAO Species Catalogue for Fishery Purposes No. 6. Rome; FAO: Rome, Italy, 2012; 150p.
9. Hasaballah, A.I.; El-Naggar, H.A. Antimicrobial activities of some marine sponges, and its biological, repellent effects against *Culex pipiens* (Diptera: Culicidae). *Ann. Res. Rev. Biol.* **2017**, *12*, 1–14. [[CrossRef](#)]
10. Cui, H.; Bashar, M.A.E.; Rady, I.; El-Naggar, H.A.; Abd El-Maoula, L.M.; Mehany, A.B.M. Antiproliferative activity, proapoptotic effect, and cell cycle arrest in human cancer cells of some marine natural product extract. *Oxid. Med. Cell. Long.* **2020**, *2020*, 7948705. [[CrossRef](#)]
11. Abo-State, M.A.; Mahdy, H.M.; Ezzat, S.M.; Abd El Shakour, E.H.; El-Bahnasawy, M.A. Antimicrobial resistance profiles of *Enterobacteriaceae* isolated from Rosetta Branch of river Nile, Egypt. *World Appl. Sci. J.* **2012**, *19*, 1234–1243.
12. Ezzat, S.M.; Abo-State, M.A.; Mahdy, H.M.; Abd EL-Shakour, E.H.; El-Bahnasawy, M.A. The effect of ionizing radiation on multi-drug resistant *Pseudomonas aeruginosa* isolated from aquatic environments in Egypt. *Br. Microbiol. Res. J.* **2014**, *4*, 856–868. [[CrossRef](#)]
13. Murray, C.J.; Ikuta, K.S.; Sharara, F.; Swetschinski, L.; Aguilar, G.R.; Gray, A.; Han, C.; Bisignano, C.; Rao, P.; Wool, E.; et al. Global burden of bacterial antimicrobial resistance in 2019: A systematic analysis. *Lancet* **2022**, *399*, 629–655. [[CrossRef](#)] [[PubMed](#)]
14. Ali, K.; Dwivedi, S.; Azam, A.; Saquib, Q.; Al-Said, M.S.; Alkhedhairi, A.A.; Musarrat, J. *Aloe vera* extract functionalized zinc oxide nanoparticles as nano antibiotics against multi-drug resistant clinical bacterial isolates. *J. Coll. Inter. Sci.* **2016**, *472*, 145–156. [[CrossRef](#)]
15. Shehabeldine, A.M.; Elbahnasawy, M.A.; Hasaballah, A.I. Green Phytosynthesis of Silver Nanoparticles Using *Echinocloa stagnina* Extract with Reference to Their Antibacterial, Cytotoxic, and Larvicidal Activities. *Bionanoscience* **2021**, *11*, 526–538. [[CrossRef](#)]
16. Pillai, A.M.; Sivasankarapillai, V.S.; Rahdar, A.; Joseph, J.; Sadeghfar, F.; Rajesh, K.; Kyzas, G.Z. Green synthesis and characterization of zinc oxide nanoparticles with antibacterial and antifungal activity. *J. Mol. Struct.* **2020**, *1211*, 128107. [[CrossRef](#)]
17. Dappula, S.S.; Kandrakonda, Y.R.; Shaik, J.B.; Mothukuru, S.L.; Lebaka, V.R.; Mannarapu, M.; Amooru, G.D. Biosynthesis of zinc oxide nanoparticles using aqueous extract of *Andrographis alata*: Characterization, optimization and assessment of their antibacterial, antioxidant, antidiabetic and anti-Alzheimer's properties. *J. Mol. Struct.* **2023**, *1273*, 134264. [[CrossRef](#)]
18. Benelli, G. Research in mosquito control: Current challenges for a brighter future. *Parasitol. Res.* **2015**, *114*, 2801–2805. [[CrossRef](#)]
19. Hasaballah, A.I. Impact of gamma irradiation on the development and reproduction of *Culex pipiens* (Diptera; Culicidae). *Int. J. Rad. Biol.* **2018**, *94*, 844–849. [[CrossRef](#)]

20. Hasaballah, A.I. Impact of paternal transmission of gamma radiation on reproduction, oogenesis and spermatogenesis of the housefly, *Musca domestica* L. (Diptera: Muscidae). *Int. J. Rad. Biol.* **2021**, *97*, 376–385. [[CrossRef](#)]
21. Chintalchere, J.M.; Dar, M.A.; Pandit, R.S. Biocontrol efficacy of bay essential oil against housefly, *Musca domestica* (Diptera: Muscidae). *J. Basic Appl. Zool.* **2020**, *81*, 6. [[CrossRef](#)]
22. Fotedar, R.; Banerjee, U.; Singh, S.; Shriniwas, A.; Verma, A.K. The house fly *Musca domestica* as a carrier of pathogenic microorganisms in a Hospital Environment. *J. Hosp. Infect.* **1992**, *20*, 209–215. [[CrossRef](#)]
23. Campbell, A.C. *Echinoderms of the Red Sea*; Edwards, A.J., Head, S.M., Eds.; Elsevier: Amsterdam, The Netherlands, 1987; pp. 215–232.
24. Cherbonnier, G. *Echinodermes: Holothurians*; IRD Editions: Paris, France, 1988; 292p.
25. Erwin, D.G.; Picton, B.E. *Guide to Inshore Marine Life*; IMMEL Publishing: London, UK, 1990; p. 219.
26. Lieske, E.; Myers, R.F. *Coral Reef Guide Red Sea: The Definitive Guide to over 1200 Species of Underwater Life*; Harper Collins Publishers: New York, NY, USA, 2004; 211p.
27. Ballantine, D.L.; Gerwick, W.H.; Velez, S.M.; Alexander, E.; Guevara, P. Antibiotic activity of lipid-soluble extracts from Caribbean marine algae. *Hydrobiologia* **1987**, *151*, 463–469. [[CrossRef](#)]
28. Kalaba, M.H.; Moghannem, S.A.; El-Hawary, A.S.; Radwan, A.A.; Sharaf, M.H.; Shaban, A.S. Green synthesized ZnO nanoparticles mediated by *Streptomyces plicatus*: Characterizations, antimicrobial and nematocidal activities and cytogenetic effects. *Plants* **2021**, *10*, 1760. [[CrossRef](#)] [[PubMed](#)]
29. Singh, M.; Kumar, M.; Kalaivani, R.; Manikandan, S.; Kumaraguru, A.K. Metallic silver nanoparticle: A therapeutic agent in combination with antifungal drug against human fungal pathogen. *Bioprocess Biosys. Eng.* **2013**, *36*, 407–415. [[CrossRef](#)] [[PubMed](#)]
30. Barzinjy, A.A.; Azeez, H.H. Green synthesis and characterization of zinc oxide nanoparticles using *Eucalyptus globulus* Labill. leaf extract and zinc nitrate hexahydrate salt. *SN Appl. Sci.* **2020**, *2*, 1–14. [[CrossRef](#)]
31. Sharaf, M.H.; Abdelaziz, A.M.; Kalaba, M.H.; Radwan, A.A.; Hashem, A.H. Antimicrobial, Antioxidant, Cytotoxic Activities and Phytochemical Analysis of Fungal Endophytes Isolated from *Ocimum basilicum*. *Appl. Biochem. Biotechnol.* **2021**, *194*, 1271–1289. [[CrossRef](#)] [[PubMed](#)]
32. Hasaballah, A.I.; El Nagggar, H.A.; Abdelbary, S.; Bashar, M.A.E.; Selim, T.A. Eco friendly Synthesis of Zinc Oxide Nanoparticles by Marine Sponge, *Spongia officinalis*: Antimicrobial and Insecticidal Activities against the Mosquito Vectors, *Culex pipiens* and *Anopheles pharoensis*. *BioNanoScience* **2021**, *12*, 89–104. [[CrossRef](#)]
33. Hasaballah, A.I.; Selim, T.A.; Tanani, M.A.; Nasr, E.E. Lethality and Vitality Efficiency of Different Extracts of *Salix safsaf* Leaves against the House Fly, *Musca domestica* L. (Diptera: Muscidae). *Afr. Entomol.* **2021**, *29*, 479–490. [[CrossRef](#)]
34. World Health Organization. *Guidelines for Laboratory and Field Testing of Mosquito Larvicides*; World Health Organization: Geneva, Switzerland, 2005; pp. 1–39.
35. Wright, J.W. The WHO Programme for the Evaluation and Testing of New Insecticides. *Bull. World Heal. Organ.* **1971**, *44*, 11–12.
36. Mount, D.I. *Methods for Aquatic Toxicity Identification Evaluations: Phase I: Toxicity Characterization Procedures*; US Environmental Protection Agency: Washington, DC, USA; Environmental Research Laboratory: Narragansett, DC, USA; National Effluent Toxicity Assessment Center United States: Duluth, MN, USA, 1988; Volume 88.
37. Al-Motabagani, M.A. Histological and histochemical studies on the effects of methotrexate on the liver of adult male albino rat. *Int. J. Morphol.* **2006**, *24*, 417–422. [[CrossRef](#)]
38. Yusof, H.; Rahman, A.; Mohamad, R.; Zaidan, U.H.; Samsudin, A.A. Biosynthesis of zinc oxide nanoparticles by cell-biomass and supernatant of *Lactobacillus plantarum* TA4 and its antibacterial and biocompatibility properties. *Sci. Rep.* **2020**, *10*, 1–13.
39. Ehsan, S.; Sajjad, M. Bioinspired synthesis of zinc oxide nanoparticle and its combined efficacy with different antibiotics against multidrug resistant bacteria. *J. Biomater. Nanobiotechnol.* **2017**, *8*, 159–175. [[CrossRef](#)]
40. El-Belely, E.F.; Farag, M.; Said, H.A.; Amin, A.S.; Azab, E.; Gobouri, A.A.; Fouda, A. Green synthesis of zinc oxide nanoparticles (ZnO NPs) using *Arthrospira platensis* (Class: Cyanophyceae) and evaluation of their biomedical activities. *Nanomaterials* **2021**, *11*, 95. [[CrossRef](#)]
41. Chaudhuri, S.K.; Malodia, L. Biosynthesis of zinc oxide nanoparticles using leaf extract of *Calotropis gigantea*: Characterization and its evaluation on tree seedling growth in nursery stage. *Appl. Nanosci.* **2017**, *7*, 501–512. [[CrossRef](#)]
42. Agarwal, H.; Nakara, A.; Menon, S.; Shanmugam, V. Eco-friendly synthesis of zinc oxide nanoparticles using *Cinnamomum Tamala* leaf extract and its promising effect towards the antibacterial activity. *J. Drug. Del. Sci. Technol.* **2019**, *53*, 101212. [[CrossRef](#)]
43. Nithya, K.; Kalyanasundharam, S. Effect of chemically synthesis compared to biosynthesized ZnO nanoparticles using aqueous extract of *C. halicacabum* and their antibacterial activity. *OpenNano* **2019**, *4*, 100024. [[CrossRef](#)]
44. Elbahnasawy, M.A.; Shehabeldine, A.M.; Khattab, A.M.; Amin, B.H.; Hashem, A.H. Green biosynthesis of silver nanoparticles using novel endophytic *Rothia endophytica*: Characterization and anticandidal activity. *J. Drug Deliv. Sci. Technol.* **2021**, *62*, 102401. [[CrossRef](#)]
45. Mohammadian, M.; Es'haghi, Z.; Hooshmand, S. Green and chemical synthesis of zinc oxide nanoparticles and size evaluation by UV-vis spectroscopy. *J. Nanomed. Res.* **2018**, *7*, 00175.
46. Jayarambabu, N.; Kumari, B.S.; Rao, K.V.; Prabhu, Y.T. Germination and growth characteristics of mungbean seeds (*Vigna radiata* L.) affected by synthesized zinc oxide nanoparticles. *Int. J. Curr. Eng. Technol.* **2014**, *4*, 2347–5161.
47. Raghunath, A.; Perumal, E. Metal oxide nanoparticles as antimicrobial agents: A promise for the future. *Int. J. Antimicrob. Agents.* **2017**, *49*, 137–152. [[CrossRef](#)]

48. Wagner, G.; Korenkov, V.; Judy, J.D.; Bertsch, P.M. Nanoparticles composed of Zn and ZnO inhibit *Peronospora tabacina* spore germination in vitro and *P. tabacina* infectivity on tobacco leaves. *Nanomaterials* **2016**, *6*, 50. [[CrossRef](#)]
49. Sirelkhatim, A.; Mahmud, S.; Seeni, A.; Kaus, N.H.M.; Ann, L.C.; Bakhori, S.K.M.; Mohamad, D. Review on zinc oxide nanoparticles: Antibacterial activity and toxicity mechanism. *Nano-Micro. Lett.* **2015**, *7*, 219–242. [[CrossRef](#)] [[PubMed](#)]
50. Tiwari, V.; Mishra, N.; Gadani, K.; Solanki, P.S.; Shah, N.A.; Tiwari, M. Mechanism of anti-bacterial activity of zinc oxide nanoparticle against carbapenem-resistant *Acinetobacter baumannii*. *Front. Microbiol.* **2018**, *9*, 1218. [[CrossRef](#)] [[PubMed](#)]
51. He, L.; Liu, Y.; Mustapha, A.; Lin, M. Antifungal activity of zinc oxide nanoparticles against *Botrytis cinerea* and *Penicillium expansum*. *Microbiol. Res.* **2011**, *166*, 207–215. [[CrossRef](#)]
52. da Silva, B.L.; Abuçafy, M.P.; Manaia, E.B.; Junior, J.A.O.; Chiari-Andréo, B.G.; Pietro, R.C.R.; Chiavacci, L.A. Relationship Between Structure And Antimicrobial Activity Of Zinc Oxide Nanoparticles: An Overview. *Int. J. Nanomed.* **2019**, *14*, 9395–9410. [[CrossRef](#)]
53. Babayevska, N.; Przysiecka, Ł.; Iatsunskiy, I.; Nowaczyk, G.; Jarek, M.; Janiszewska, E.; Jurga, S. ZnO size and shape effect on antibacterial activity and cytotoxicity profile. *Sci. Rep.* **2022**, *12*, 8148. [[CrossRef](#)]
54. Hasaballah, A.I.; Gobara, I.M.; El-Naggar, H.A. Larvicidal activity and ultrastructural abnormalities in the ovaries of the housefly “*Musca domestica*” induced by the soft coral “*Ovabunda macrospiculata*” synthesized ZnO nanoparticles. *Egypt. J. Aquat. Biol. Fish.* **2021**, *25*, 721–738. [[CrossRef](#)]
55. Cengiz, E.I.; Unlu, E. Sublethal effects of commercial deltamethrin on the structure of the gill, liver and gut tissues of mosquitofish, *Gambusia affinis*: A microscopic study. *Environ. Toxicol. Pharmacol.* **2006**, *21*, 246–253. [[CrossRef](#)] [[PubMed](#)]
56. Tilak, K.S.; Veeraiyah, K.; Yacobu, K. Studies o histopathological changes in the gill, liver and kidney of *Ctenopharyngodon idellus* (Valenciennes) exposed to technical fenvalerate and EC 20%. *Pollut. Res.* **2001**, *20*, 387–393.
57. Ikele, C.B.; Mgbenka, B.O.; Oluah, N.S. Histopathological effects of diethyl phthalate on *Clarias gariepinus* juveniles. *Anim. Re. Inter.* **2011**, *8*, 1431–1438.
58. Sarkar, B.; Chatterjee, A.; Adhikari, S.; Ayyappan, S. Carbofuran- and cypermethrin-induced histopathological alterations in the liver of *Labeo rohita* (Hamilton) and its recovery. *J. Appl. Ichthyol.* **2005**, *21*, 131–135. [[CrossRef](#)]
59. Kaya, H.; Duysak, M.; Akbulut, M.; Yılmaz, S.; Gürkan, M.; Arslan, Z.; Ateş, M. Effects of subchronic exposure to zinc nanoparticles on tissue accumulation, serum biochemistry, and histopathological changes in tilapia (*Oreochromis niloticus*). *Environ. Toxicol.* **2017**, *32*, 1213–1225. [[CrossRef](#)] [[PubMed](#)]
60. Zhu, X.; Zhu, L.; Duan, Z.; Qi, R.; Li, Y.; Lang, Y. Comparative toxicity of several metal oxide nanoparticle aqueous suspensions to zebra fish (*Danio rerio*) early developmental stage. *J. Environ. Sci. Health A* **2008**, *43*, 278–284. [[CrossRef](#)] [[PubMed](#)]
61. Zhu, X.; Wang, J.; Zhang, X.; Chang, Y.; Chen, Y. The impact of ZnO nanoparticle aggregates on the embryonic development of zebrafish (*Danio rerio*). *Nanotechnology* **2009**, *20*, 195103. [[CrossRef](#)] [[PubMed](#)]
62. Hao, L.; Chen, L. Oxidative stress responses in different organs of carp (*Cyprinus carpio*) with exposure to ZnO nanoparticles. *Ecotoxicol. Environ. Saf.* **2012**, *80*, 103–110. [[CrossRef](#)]

**Disclaimer/Publisher’s Note:** The statements, opinions and data contained in all publications are solely those of the individual author(s) and contributor(s) and not of MDPI and/or the editor(s). MDPI and/or the editor(s) disclaim responsibility for any injury to people or property resulting from any ideas, methods, instructions or products referred to in the content.